**Supporting Information**

# Pellet-fed gasifier stoves approach gas-stove like performance during in-home use in Rwanda

Champion, Wyatt M.[1,#], and Grieshop, Andrew P.[1*]
1. Department of Civil, Construction, and Environmental Engineering, North Carolina State University, Raleigh, North Carolina 27695, United States
# Current affiliation: Oak Ridge Institute for Science and Education (ORISE), U.S. Environmental Protection Agency, Office of Research and Development, Research Triangle Park, North Carolina 27709, United States

* Address correspondence to:

Andrew P. Grieshop, Department of Civil, Construction, and Environmental Engineering, North Carolina State University, 431B Mann Hall, Raleigh, NC 27696-7908, USA. Email: apgriesh@ncsu.edu; Ph. +1 (919) 513-1181

**Total Pages: 21**

**Number of Figures 15; Number of Tables: 7**

## SI CONTENTS



## Section S1. Filter analysis and data quality assurance

Teflon filters (47 mm Zefon Zefluor, 2 micron pore size) were weighed before and after the campaign using a microbalance (Mettler Toledo UMX-2) to derive gravimetric $PM_{2.5}$ concentrations for each test. Teflon filters were equilibrated in the weighing chamber with controlled temperature (22±2°C) and RH (35±2.5%) for 24 hours and charge neutralized with Polonium and electrostatic ionization sources before weighing. Field blank filters (n=7) were used to correct gravimetric $PM_{2.5}$ concentrations. Quartz fiber filters were pre-baked in a laboratory oven at 550°C for 24 hours and stored in Petri dishes lined with baked aluminum foil before and after sampling. Organic and Elemental Carbon (OC/EC) analysis of quartz fiber filters with a Sunset OC/EC Analyzer used a modified NIOSH thermo-optical transmission (TOT) protocol with longer step durations to ensure complete removal of OC on heavily loaded filters. Table S3 gives the details of the protocol. Gas sensor calibrations were performed before and after the field campaign using custom calibration gas cylinders (Airgas). Flows were regularly checked in the field with a rotameter or primary flow calibrator (Drycal Defender 510). The light scattering sensor in the STEMS was calibrated with emissions from a 'rocket' style cookstove in the laboratory against a Photoacoustic Extinctiometer (PAX) at 870 nm with a $R^2$=0.68. The PAX was calibrated using atomized ammonium sulfate and Aquadag as scattering and absorption standards, respectively. CO sensor cross-sensitivity with denatured alcohol used for system cleaning was observed in a subset of tests during the first deployment. This artifact was corrected by fitting a

Gaussian curve to the portion of data affected in the first portion of the test, and subtracting this estimated value from sensor responses. This approach was chosen so that stove CO emissions during the affected period (~15 minutes near the beginning of testing) could still be quantified.

**Section S2. Black Carbon loading correction**

For filter based optical measurement of BC, the attenuation of light (ATN) is given by,

$$ATN = 100 * \ln\left(\frac{I_0}{I}\right) \quad (1)$$

Where $I_0$ and I are light intensities through a reference blank spot and spot of aerosol on the filter ticket respectively. The factor 100 is for convenience. Particle absorption ($B_{ap}$) is calculated by the following equation:

$$B_{ap} = BC * \sigma_{ATN} = \frac{10^6 * A * \Delta ATN}{100 * Q * \Delta t} \quad (2)$$

where BC is the black carbon concentration in µg $m^{-3}$, A is the area of the sample spot ($7.1 \times 10^{-6}$ $m^2$ for the microAeth); Q is the volumetric flow rate in $m^3\ s^{-1}$; $\Delta t$ is the sampling interval in s; $\Delta ATN$ is the variation in the ATN during the period $\Delta t$, and $\sigma_{ATN}$ is the apparent mass attenuation cross-section (MAC) for the black carbon that is collected on the filter in $m^2\ g^{-1}$. MAC for the AE-51 is 12.5 $m^2\ g^{-1}$.

Filter based optical measurement of BC is associated with loading effects. At low ATN values, the relationship between ΔATN is proportional to the BC concentration on the filter. As ATN increases, the measured BC concentration (or absorption) becomes underestimated [1,2]. Absorption from AE-51 was corrected for filter loading artifacts using the approach by Park et al. (2010). For this approach, the corrected absorption is given by:

$$B_{ap}(compensated) = (1 + k * ATN) * B_{ap}(non - compensated) \quad (3)$$

In this approach, the average BC concentration in an ATN width of 2 is plotted and the factor k is calculated based on the ratio of the slope and intercept obtained from the linear fit of the plotted data. The basic idea behind this approach is that within a large data set, the probability of BC lying in an ATN bin same across all ATN bins, i.e., the BC vs ATN slope should be close to zero (Park et al. 2010). The median $B_{ap}$ value increased by 24% upon loading correction of all sessions.

## Section S3. Emission factors, emission rates, and uncertainty analysis

Emission Factors were estimated by the carbon balance method, which assumes that the carbon fraction of fuel (47.5%, 45.4%, and 81.9% for pellet, wood, and charcoal fuels, respectively) by weight is emitted as gaseous carbon ($CO + CO_2$), as shown in equation (4).

$$Pollutant\ EF\left(\frac{g}{kg}\right) = \frac{Pollutant\ concentration\ (g\ m^{-3})}{\Delta CO + \Delta CO_2(mol\ C\ m^{-3}) * 0.012(\frac{kg\ C}{mol\ C})} * f_C(\frac{kg\ C}{kg\ fuel}) \quad (4)$$

Where $\Delta$ represents background corrected concentrations, and $f_c$ is the carbon fraction of the fuel by weight. Conversion from ppm to mol C $m^{-3}$ was via the ideal gas law, where temperature from the STEMS was used.

The average emission rate for a cooking session was determined by equation (5) where EF is determined by carbon balance and dry fuel consumed is the weight of the fuel with measured water weight subtracted.

$$Emission\ Rate\ (mg\ \mathrm{min}^{-1}) = EF(g\ kg^{-1}) * \frac{Dry\ wood\ consumed\ (kg)}{Cooking\ duration\ (\mathrm{min})} * 1000\frac{mg}{g} \quad (5)$$

Measurement uncertainties incorporated into this work are listed in Table S4 below. The uncertainties in calculated quantities were calculated using standard error propagation approaches. Median relative uncertainties (± IQR) for $PM_{2.5}$ and CO EFs were 14.0% (± 8.3%) and 38.7% (± 70.1%). $PM_{2.5}$ EF uncertainties were typical of previous field work [4], while CO EFs were higher due to the relatively clean performance of the Pellet stoves resulting in low background-corrected CO signal (e.g., median value of 7.2 ppm for Pellet tests) compared to the absolute uncertainty of the CO sensor (5 ppm).

SSA in this study was calculated from absorption at 880 nm and scattering at 870 nm. However, the resulting difference in scattering is less than 5% between these wavelengths for the usual Angstrom exponent values (from AAE = 1-3), and therefore is within uncertainty bounds for scattering.

## Section S4. PaRTED analysis

The instantaneous scattering emission factor ($IEF_{scat}$) represents the amount of light scattering related to the particulate matter emissions from the combustion of 1 kg of fuel. The $IEF_{scat}$ for each combustion event was estimated using the following equation:

$$IEF_{scat,i} = B_{sp,i}/C_{carbon,i} \qquad (6)$$

Where:

$B_{sp,i}$ = scattering coefficient ($Mm^{-1}$)

$C_{carbon}$ = background corrected carbon concentration (ppm)

$IEF_{scat,i}$ = instantaneous scattering emission factor ($m^2\ kg^{-1}$ wood)

Additional information on calculations can be found in the manuscript and supporting information of Chen et al. (2012). The $IEF_{scat}$ is a proxy for the relationship between light scattering and mass concentration during a combustion event based on the fuel usage.

## Section S5. Global warming commitment (GWC) and PM intake calculations

Baseline household fuel consumption (2.41 tonne $yr^{-1}$) was based on average household size in Rwanda (4.3 ppl $house^{-1}$) [6], average annual per capita dry fuelwood consumption in Rwanda (486 kg dry-wood $ppl^{-1}\ yr^{-1}$) [7], and the average wood moisture content observed in the present study (13.4%). We applied this to calculate our baseline energy demand assuming that the baseline technology is a TSF with thermal efficiency of 14.1% [8]. Assuming a wood heating value of 15.1 MJ $kg^{-1}$, a daily energy use of 14.0 MJ $day^{-1}$ $stove^{-1}$ was calculated and set as a baseline for further calculations. Fuel savings were calculated relative to this baseline using the reductions in average fuel consumption rate (in kg $hr^{-1}$) for the stoves studied in this work. The pellet stove reduced mean fuel usage by 73.9%.

The GWC is calculated by the equation:

$$GWC = \sum(GWP_i * AE_i) \qquad (7)$$

Where, $GWP_i$ is the 100 year global warming potential for each species ($CO_2$, CO, OC, BC/EC and $CH_4$) and $AE_i$ is the mass of pollutant emitted per year. GWP values were taken from the IPCC 2013 report [9] are listed in Table S5. LPG stoves were assumed to have a thermal efficiency of 53.6% and the fuel a heating value of 45.8 MJ $kg^{-1}$ [10].

Cobenefit calculations for pellet, charcoal, and LPG stove types included upstream emissions associated with the production of the fuel. For pellet stoves, three scenarios were modeled: 1) hydroelectric power supply and default non-renewable biomass fraction, 2) hydroelectric power supply and "completely renewable" biomass fraction (i.e., pellet feedstock is considered 100% renewable), and 3) diesel generator and default non-renewable biomass fraction. Pellet upstream emissions from diesel generators were based on an in-house estimate of electricity demand from pellet production specific to Inyenyeri (0.32 MW-hr tonne-pellet$^{-1}$), and fleet-average emission factors from diesel backup generators [11], as summarized in Table S6. Pellet upstream GWC (defined as feedstock production and fuel processing) were 15% of the in-use combustion contribution, agreeing closely with a value of 14% from a life cycle assessment of biomass production in Kenya [12]. For charcoal, upstream emissions were derived from measurements of a Kenyan charcoal kiln [13,14]. Our estimates for charcoal upstream emissions (146% of use-phase) are lower than the US EPA (2017) estimates for charcoal production in Kenya (315% of the in-use combustion 100 year GWC based on greenhouse gas and short-lived climate forcing emissions). Upstream LPG emissions were assumed to be 41% of combustion emissions based on LPG data from the same life cycle assessment for Kenya [12].

An individual intake fraction of 1300 ppm was used to link PM emissions to intake as in Grieshop et al. (2011). This calculation of health risk was updated to apply the dose-response relationship from [15] to estimate adjusted relative risk of all-age mortality due to ischemic heart disease associated with this PM intake.

**Table S1.** Assumed Fuel Energy Contents Used in Cobenefit Modeling [14]

| Fuel Type | Energy Content (MJ $kg^{-1}$) |
|---|---|
| Pellet | 17.3 |
| Wood | 15.1 |
| Charcoal | 25.7 |
| LPG | 45.8 |

**Table S2.** Assumed Stove Thermal Efficiencies Used in Cobenefit Modeling

| Stove Type | Thermal Efficiency (%) | Reference | Reference Stove Type |
|---|---|---|---|
| LPG | 53.6 | [10] | LPG |
| Wood Forced Draft | 38.9 | [8] | Philips HD4012 Fan |
| Wood Gasifier | 34.0 | [8] | Philips HD4008 Natural Draft |
| Wood Rocket | 34.8 | [8] | StoveTec GreenFire |
| Wood Three Stone Fire | 14.1 | [8] | Three Stone Fire, carefully and minimally attended |
| Pellet | 46.8 | [16] | Mimi Moto |
| Wood | 14.1 | Same as “Wood Three Stone Fire” above | Same as “Wood Three Stone Fire” above |
| Charcoal | 24.4 | [8] | Jiko Ceramic |

**Table S3.** Temperature protocol for OC/EC analysis, Sunset Laboratory Analyzer

| Mode | Time (s) | Temperature (°C) | Power Constant | Time Constant (s) | Blower Mode |
|---|---|---|---|---|---|
| Helium | 10 | 1 | 0.001 | 100 | 0 |
| Helium | -1 | 200 | 0.055 | 85 | 0 |
| Helium | -1 | 310 | 0.055 | 85 | 0 |
| Helium | -1 | 475 | 0.095 | 75 | 0 |
| Helium | -1 | 615 | 0.15 | 45 | 0 |
| Helium | -1 | 700 | 0.3 | 35 | 0 |
| Helium | -1 | 550 | 0.001 | 100 | 16 |
| Oxygen | 90 | 550 | 0.18 | 65 | 0 |
| Oxygen | 90 | 625 | 0.18 | 42 | 0 |
| Oxygen | 90 | 700 | 0.2 | 36 | 0 |
| Oxygen | 90 | 775 | 0.27 | 32 | 0 |
| Oxygen | 90 | 850 | 0.25 | 25 | 0 |
| Oxygen | -1 | 871 | 0.3 | 20 | 0 |
| CalibrationOx | 120 | 1 | 0.001 | 100 | 16 |
| Offline | 1 | 0 | 0.001 | 100 | 16 |

Note: Time of -1 indicates that the FID should return to baseline.

**Table S4.** Summary of measurement uncertainties. Values taken from sensor specification sheets.

| Sensor | Manufacturer/Model | Uncertainty | Notes |
|---|---|---|---|
| **$CO_2$** | Cozir NDIR Ambient | 40 ppm ± 3% reading | Uncertainty propagated along with pre- and post-calibration in laboratory |
| **CO** | Electrochemical | 5 ppm ± 2% reading | Uncertainty propagated along with pre- and post-calibration in laboratory |
| **Filter flows** | Honeywell AWM5101 | 3% | Uncertainty propagated along with pre- and post-calibration in laboratory |
| **AE-51 flow** | Honeywell AWM 3150V | 3% | Uncertainty propagated along with pre- and post-calibration in laboratory |
| **Temperature** | Texas Instrument LM35 | 2°C | |
| **Wood weight** | na | 20% | To account for un-weighed char after cooking session. |
| **OC/EC** | Sunset Labs | As reported by Sunset OC/EC analyzer | |
| **STEMS scattering cell** | Aprovecho PEMS Board | Calibrated against PAX at 870 nm | Uncertainty propagated along with pre- and post-calibration in laboratory |
| **AE-51 absorption** | Aethlabs | 1.25 $Mm^{-1}$ | Reported uncertainty of AE-51 is 0.1 $\mu g\ m^{-3}$, assumed mass absorption cross-section (MAC) is 12.5 $m^2\ g^{-1}$. Propagated with uncertainty from AE-51 flowmeter. |
| **Wood carbon content** | na | 2% | Taken from [17] |
| **Non $CO+CO_2$ contribution to carbon balance** | na | 2.5% | Taken from [17] |

**Table S5.** 100 year Global Warming Potential Values from Intergovernmental Panel on Climate Change (2013)

| Species | GWP 100 Year |
|---|---|
| $CO_2$ | 1 |
| CO | 1.9 |
| BC/EC | 658.6 |
| OC | -66.4 |
| $CH_4$ | 28.5 |

**Table S6.** Diesel Generator Emission Factors for Pellet Production [11]

| Pollutant | Emission Factor (g $kW\text{-}hr^{-1}$) |
|---|---|
| PM | 0.22 |
| OC[1] | $=0.355*EF_{PM}$ |
| EC[1] | $=0.525*EF_{PM}$ |
| CO | 1.32 |
| $CO_2$ | 806 |
| THC | 0.48 |
| $NO_x$ | 10.3 |

1. Based on load-average PM OC and EC from a non-road diesel generator [18]. Across a range of loads (0-75 kW) and for low-sulfur diesel fuel, average EC:PM ranged from 21-84% and TC:PM ranged from 83-91%.

**Table S7.** Comparison Study PM and CO Emission Factor Confidence Intervals

| Study Index | Fuel Type | PM EF CI ($g\ kg^{-1}$) | CO EF CI ($g\ kg^{-1}$) | Reference |
|---|---|---|---|---|
| Wood | Elephant Grass/Eucalyptus | 11.3, 22.5 | 100, 141 | This study |
| W1 | Varied | 5.1, 5.3 | 89.7, 105 | Roden et al. (2009) [19] |
| W2 | na | 5.6, 18.4 | 81.0, 145 | Garland et al. (2017) [20] |
| W3 | Wood/Crop Residue | 0.9, 7.5 | 49.7, 90.3 | Coffey et al. (2017) [21] |
| W4 | na | 4.9, 10.7 | 72.0, 124 | Wathore, Mortimer, and Grieshop (2017) [4] |
| W5 | na | 3.0, 10.0 | 69.9, 157 | Rose Eilenberg et al. (2018) [22] |
| W7 | na | 3.6, 10.9 | 62.7, 103 | Grieshop et al. (2017) [23] |
| Charcoal | na | 1.8, 13.8 | 307, 382 | This study |
| C1 | na | 0.4, 1.2 | 140, 234 | Coffey et al. (2017) [21] |
| C2 | na | 1.4, 11.9 | 295, 491 | Lefebvre (2016) [24] |
| C3 | na | 0.1, 6.1 | 197, 288 | Rose Eilenberg et al. (2018) [22] |


**Figure S1.** Representative Photos of Stove Types Tested (Photos: Wyatt Champion)

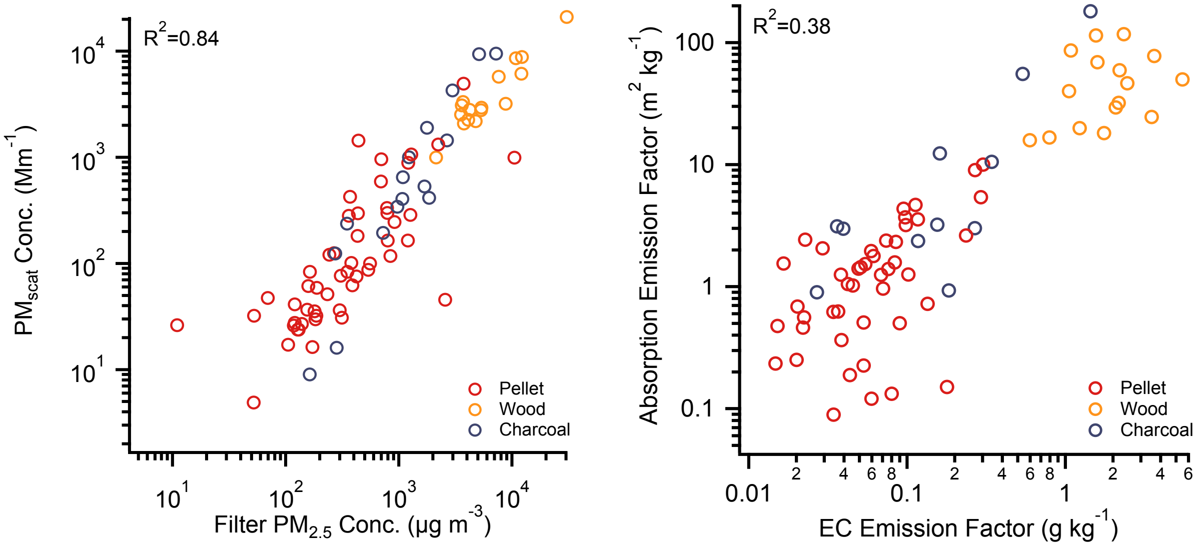


**Figure S2.** Scatter plots of (a) Mass Scattering Coefficient (MSC) and (b) Mass Absorption Coefficient (MAC) with $R^2$ values based on raw (i.e., not log-transformed) data.

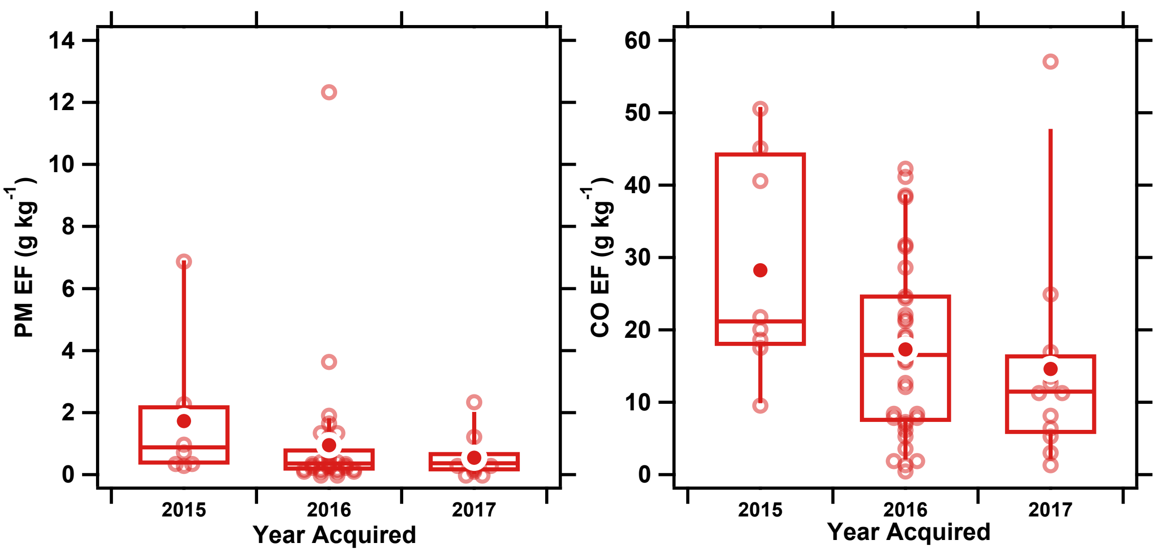


**Figure S3.** Box and whisker with jitter plots for Pellet $PM_{2.5}$ and CO EFs grouped by year that stove was acquired. One-tail Wilcoxon tests ($\alpha$=0.05) conducted within PM and CO EFs ($g\ kg^{-1}$) and between each year acquired (2015, 2016, 2017) were conducted. For both PM and CO EFs, significant differences were observed between 2015 and 2016 (p=0.02; p=0.02, respectively), 2015 and 2017 (p=0.02; p=0.01, respectively); no significant difference was observed between 2016 and 2017 (p=0.35; p=0.16, respectively). This simple analysis suggests that a pellet stove $\geq$ 2 years old may have higher PM and CO EFs.

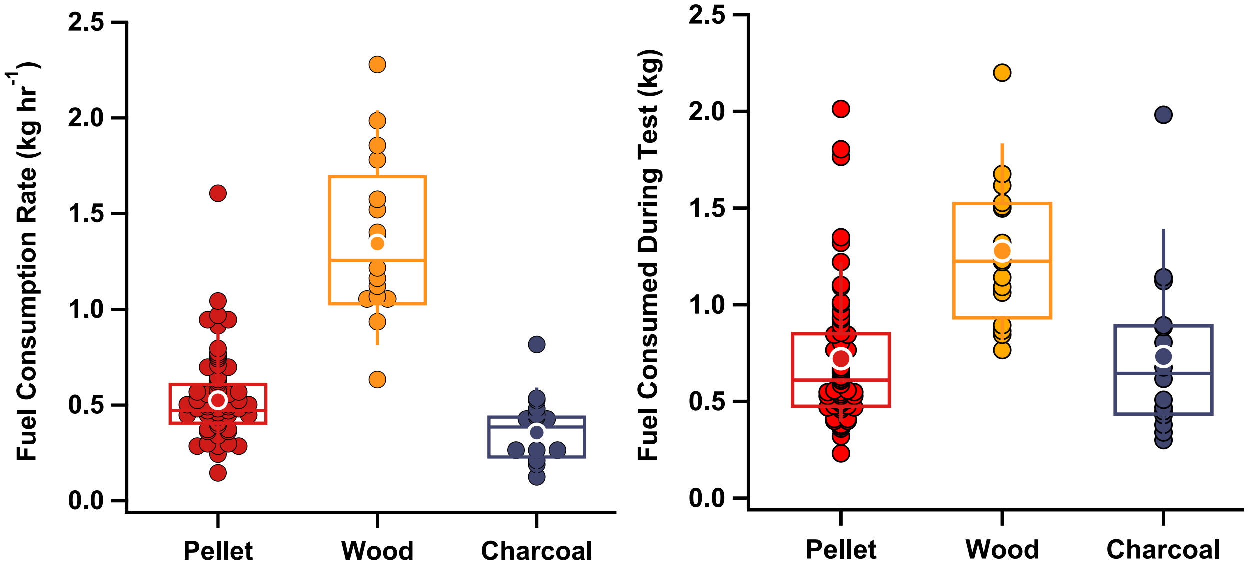


**Figure S4.** Box and whisker with jitter plots of fuel consumption rate (kg $hr^{-1}$) and fuel consumed (kg) for single cooking sessions. Mean values plotted as outlined dot, while median and IQRs plotted as box with 10/90$^{th}$ percentiles as whiskers. Fuel consumption rate is determined by dividing the wood used in a cooking task by the time required for cooking (as plotted in Figure S5).

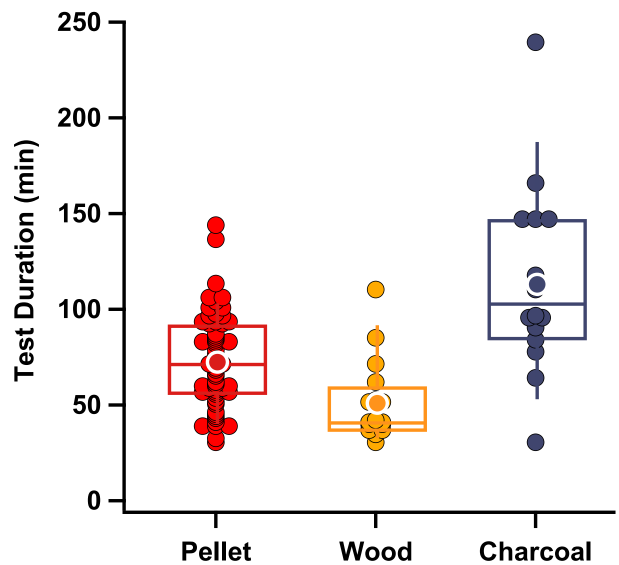


**Figure S5.** Box and whisker with jitter plot of test duration (min) for single cooking sessions.

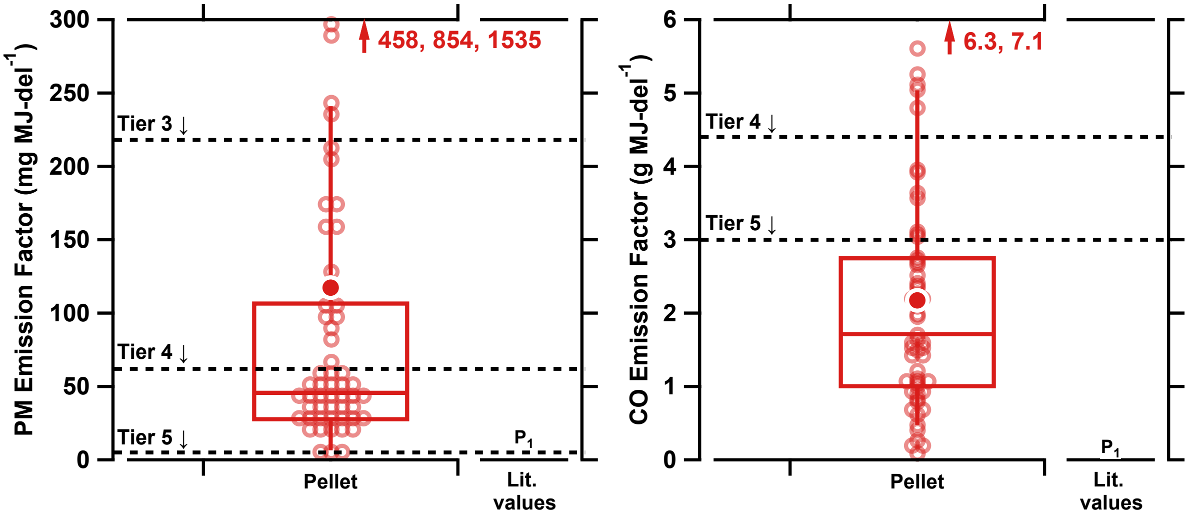


**Figure S6.** Closeup of $PM_{2.5}$ and CO emission rates for Pellet stoves with revised ISO/IWA tiers designated as horizontal dashed lines.

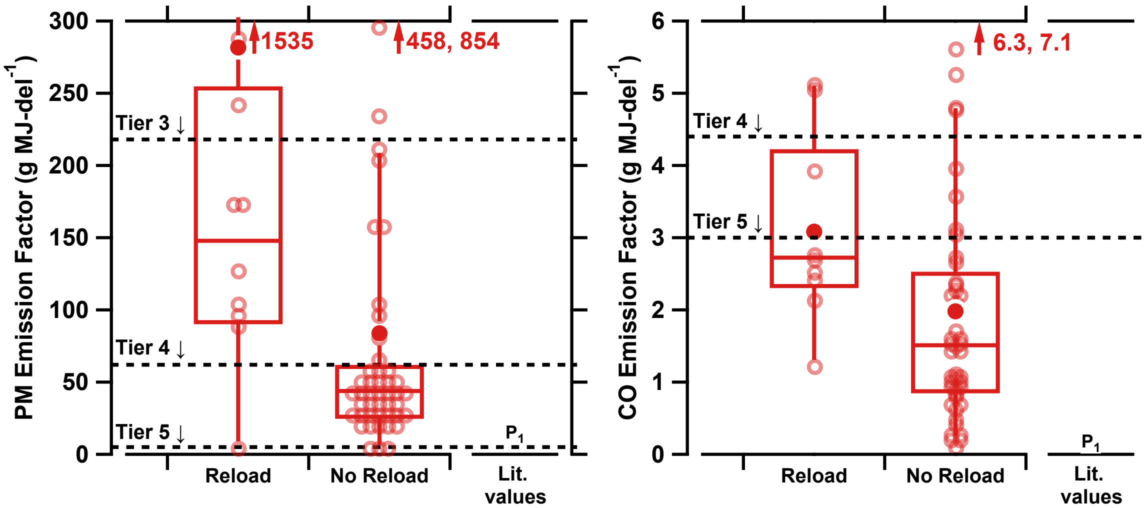


**Figure S7.** Closeup of $PM_{2.5}$ and CO emission rates for Pellet stoves with and without reload (i.e., refuel), with revised ISO/IWA tiers designated as horizontal dashed lines. Mean (and standard deviations) of pellet PM EFs with and without reloading are: 2.3 (3.6) and 0.7 (1.1) g kg$^{-1}$, respectively. Median (and IQRs) of pellet EFs with and without reloading are: 1.2 (1.1) and 0.4 (0.3) g kg$^{-1}$, respectively. For both pollutants, no reload EFs were significantly lower than for reload ($p < 0.01$).

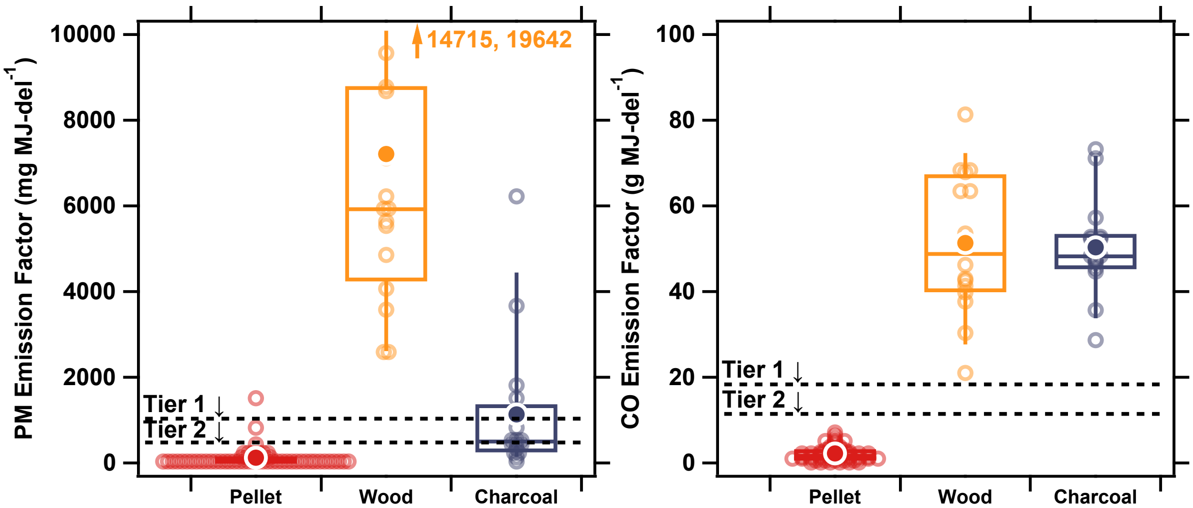


**Figure S8.** $PM_{2.5}$ and CO EFs box and whisker with jitter plots showing revised ISO/IWA tiers.

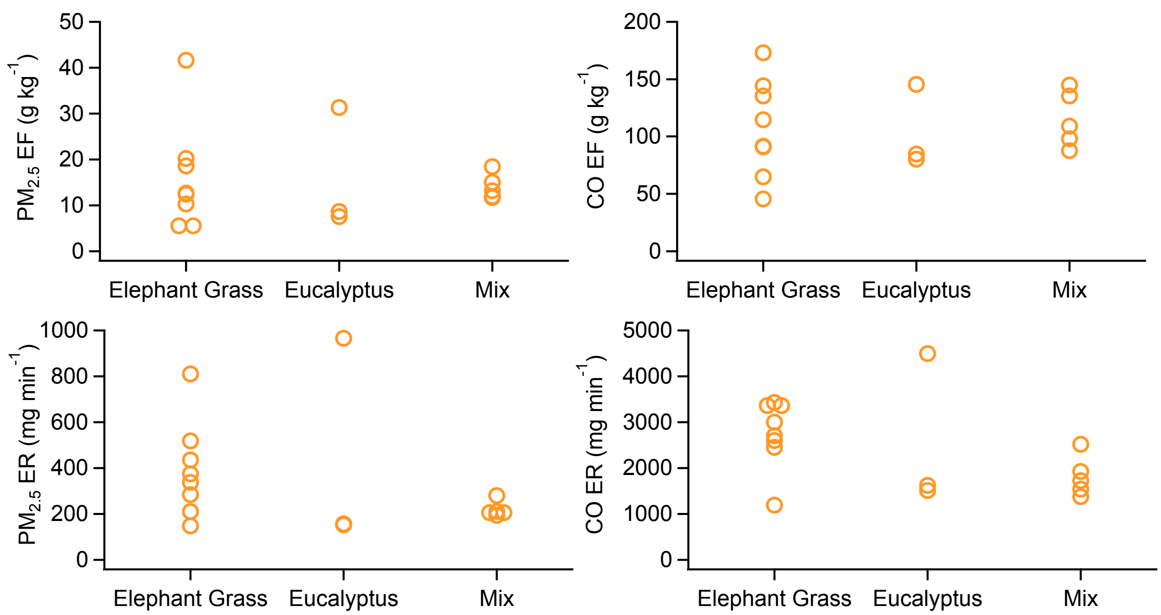


**Figure S9.** $PM_{2.5}$ and CO EFs and ERs for wood homes burning: elephant grass only, eucalyptus only, or a mix of the two fuels. Compared to mixed-wood homes, elephant grass homes had 77% and 52% higher mean $PM_{2.5}$ and CO ERs, respectively.

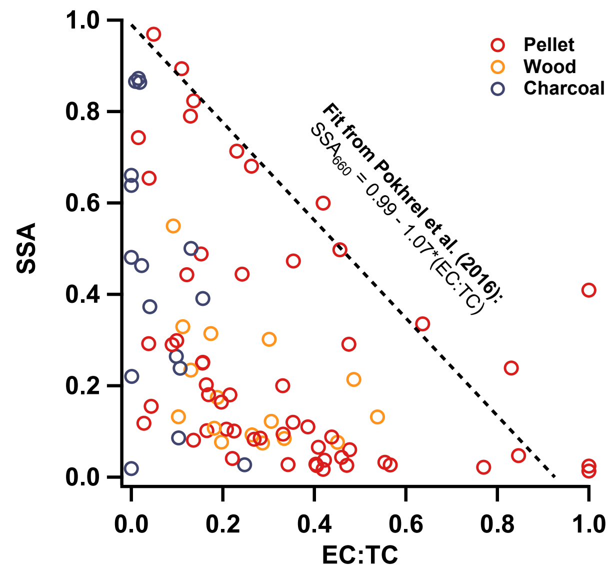


**Figure S10.** Scatterplot of SSA vs EC:TC ratio with parameterization for $SSA_{660}$ from Pokhrel et al. (2016).

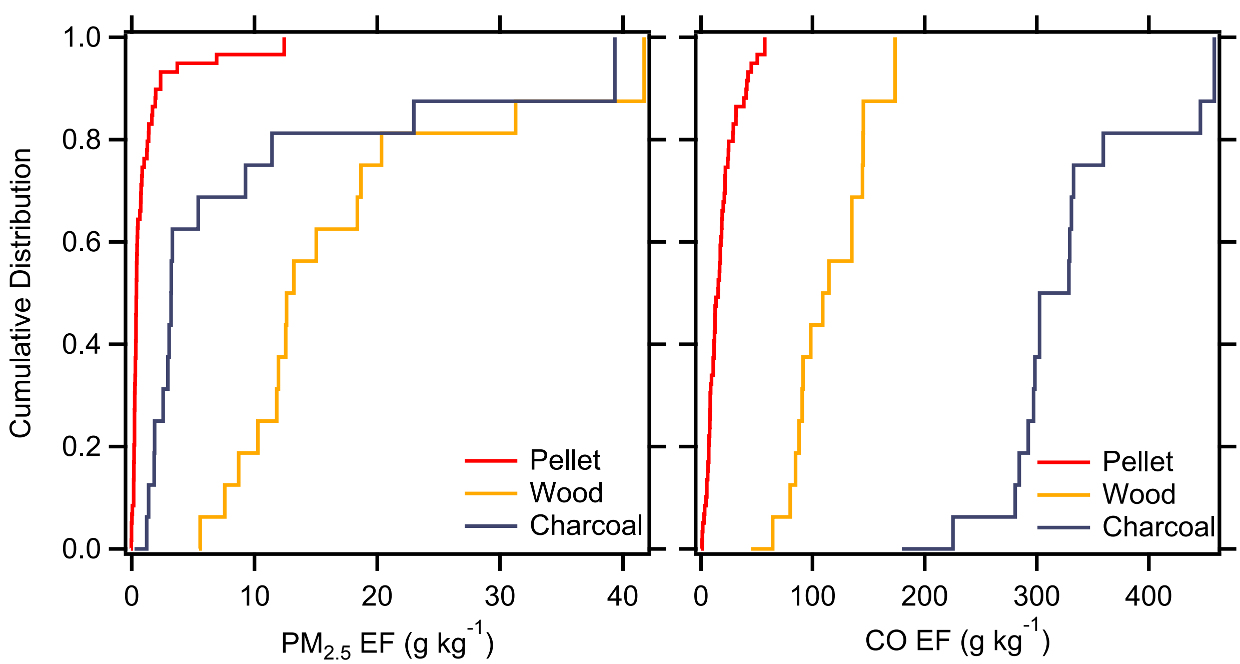


**Figure S11.** Cumulative distribution functions of $PM_{2.5}$ and CO EFs.

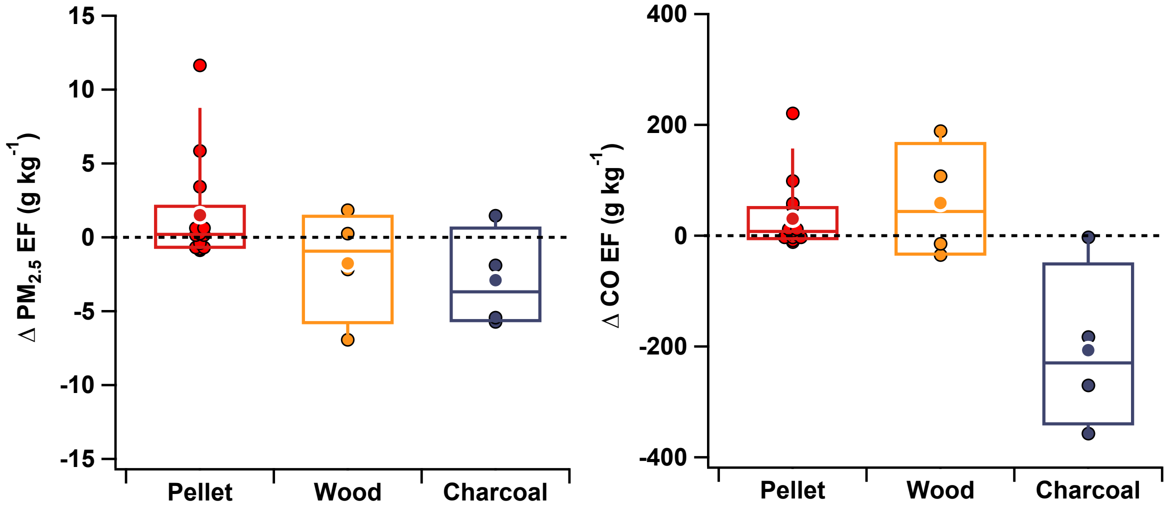


**Figure S12.** Box and whisker with jitter plots of delta $PM_{2.5}$ and CO EFs for the same households across both deployments, where delta is the difference between deployment 2 and deployment 1.

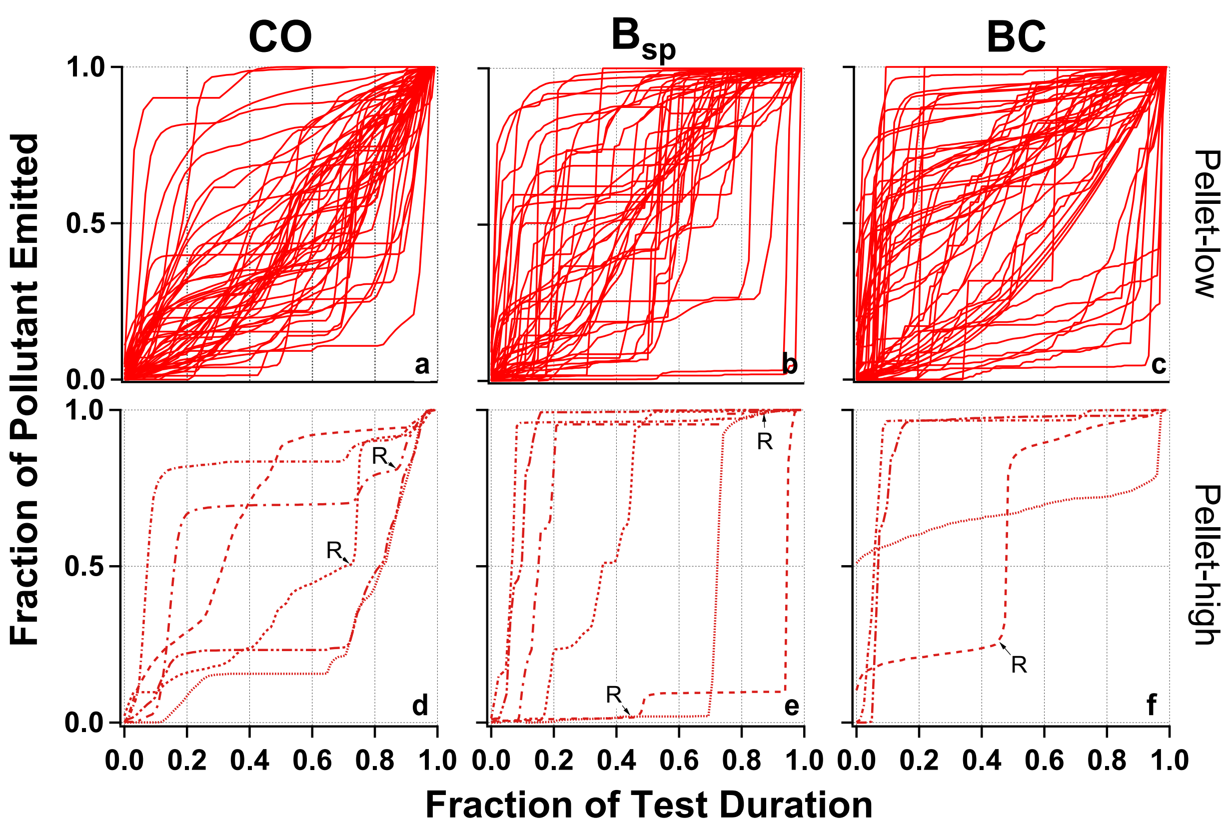


**Figure S13.** Individual CDF traces of CO, $B_{sp}$, and BC for Pellet-low and Pellet-high tests, with reload events for Pellet-high tests labeled with "R" tags.

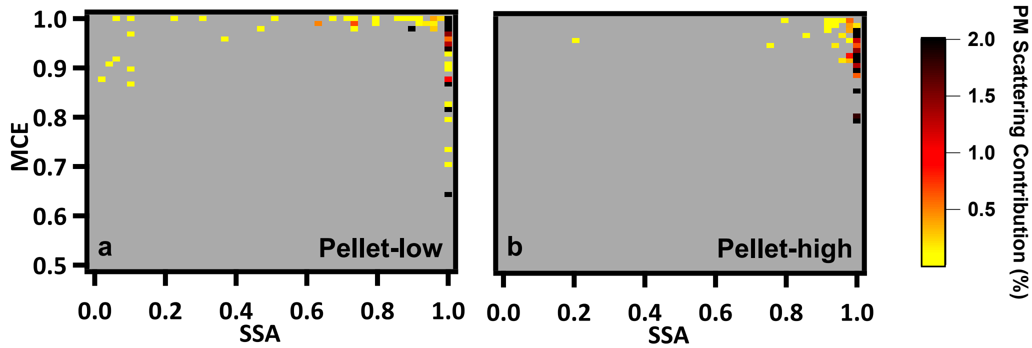


**Figure S14.** PaRTED plots weighted by PM scattering for (a) Pellet-low and (b) Pellet-high tests.

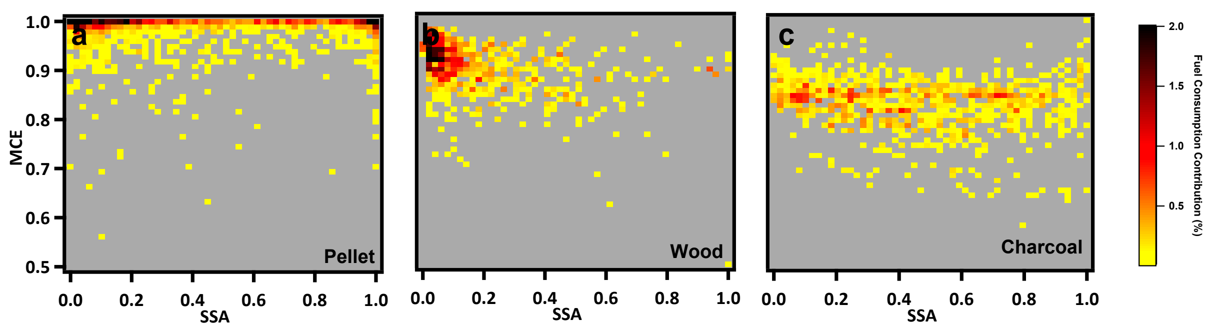


**Figure S15.** PaRTED plots weighted by fuel consumption rather than by particle scattering for (a) Pellet, (b) Wood, and (c) Charcoal Tests.

## References

(1) Gundel, L. A.; Dod, R. L.; Rosen, H.; Novakov, T. The Relationship between Optical Attenuation and Black Carbon Concentration for Ambient and Source Particles. *Sci. Total Environ.* **1984**, *36*, 197–202.

(2) Hansen, A. D. .; Rosen, H.; Novakov, T. The Aethalometer - An Instrument for the Real-Time Measurement of Optical Absorption by Aerosol Particles. *Sci. Total Environ.* **1984**, *36*, 191–196.

(3) Park, S. S.; Hansen, A. D. A.; Cho, S. Y. Measurement of Real Time Black Carbon for Investigating Spot Loading Effects of Aethalometer Data. *Atmos. Environ.* **2010**, *44* (11), 1449–1455. https://doi.org/10.1016/j.atmosenv.2010.01.025.

(4) Wathore, R.; Mortimer, K.; Grieshop, A. P. In-Use Emissions and Estimated Impacts of Traditional, Natural- and Forced-Draft Cookstoves in Rural Malawi. *Environ. Sci. Technol.* **2017**, *51* (3), 1929–1938. https://doi.org/10.1021/acs.est.6b05557.

(5) Chen, Y.; Roden, C. A.; Bond, T. C. Characterizing Biofuel Combustion with Patterns of Real-Time Emission Data (PaRTED). *Environ. Sci. Technol.* **2012**, *46* (11), 6110–6117. https://doi.org/10.1021/es3003348.

(6) United Nations. Household Size and Composition Around the World. **2017**, 1. https://doi.org/10.1007/JHEP05(2012)157.

(7) Ndayambaje, J. D.; Mohren, G. M. J. Fuelwood Demand and Supply in Rwanda and the Role of Agroforestry. *Agrofor. Syst.* **2011**, *83* (3), 303–320. https://doi.org/10.1007/s10457-011-9391-6.

(8) Jetter, J.; Zhao, Y.; Smith, K. R.; Khan, B.; Yelverton, T.; Decarlo, P.; Hays, M. D. Pollutant Emissions and Energy Efficiency under Controlled Conditions for Household Biomass Cookstoves and Implications for Metrics Useful in Setting International Test Standards. *Environ. Sci. Technol.* **2012**, *46* (19), 10827–10834. https://doi.org/10.1021/es301693f.

(9) Intergovernmental Panel on Climate Change. *Climate Change 2013: The Physical Science Basis: Working Group I Contribution to the Fifth Assessment Report of the Intergovernmental Panel on Climate Change*; 2013.

(10) Smith, K. R.; Uma, R.; Kishore, V. V. N.; Zhang, J.; Joshi, V.; Khalil, M. A. K. Greenhouse Implications of Household Stoves: An Analysis for India. *Annu. Rev. Energy Environ.* **2000**, *25* (1), 741–763. https://doi.org/10.1146/annurev.energy.25.1.741.

(11) Shah, S. D.; Cocker, D. R.; Johnson, K. C.; Lee, J. M.; Soriano, B. L.; Wayne Miller, J. Emissions of Regulated Pollutants from In-Use Diesel Back-up Generators. *Atmos. Environ.* **2006**, *40* (22), 4199–4209. https://doi.org/10.1016/j.atmosenv.2005.12.063.

(12) US EPA. *Life Cycle Assessment of Cookstove Fuels in India, China, Kenya and Ghana*; 2017.

(13) Pennise, D. M.; Smith, K. R.; Kithinji, J. P.; Rezende, M. E.; Raad, T. J.; Zhang, J.; Fan, C. Emissions of Greenhouse Gases and Other Airborne Pollutants from Charcoal Making in Kenya and Brazil. *J. Geophys. Res. Atmos.* **2001**, *106* (D20), 24143–24155.

(14) Grieshop, A. P.; Marshall, J. D.; Kandlikar, M. Health and Climate Benefits of Cookstove Replacement Options. *Energy Policy* **2011**, *39* (12), 7530–7542. https://doi.org/10.1016/j.enpol.2011.03.024.

(15) Burnett, R. T.; Pope, C. A.; Ezzati, M.; Olives, C.; Lim, S. S.; Mehta, S.; Shin, H. H.; Singh, G.; Hubbell, B.; Brauer, M.; Anderson, H. R.; Smith, K. R.; Balmes, J. R.; Bruce, N. G.; Kan, H.; Laden, F.; Prüss-Ustün, A.; Turner, M. C.; Gapstur, S. M.; Diver, W. R.; Cohen, A. An Integrated Risk Function for Estimating the Global Burden of Disease Attributable to Ambient Fine Particulate Matter Exposure. *Environ. Health Perspect.* **2014**, *122* (4), 397–403. https://doi.org/10.1289/ehp.1307049.

(16) Clean Cooking Alliance. Clean Cooking Catalog: Mimi Moto http://catalog.cleancookstoves.org/stoves/434 (accessed Feb 9, 2018).

(17) Roden, C. A.; Bond, T. C.; Conway, S.; Osorto Pinel, A. B. Emission Factors and Real-Time Optical Properties of Particles Emitted from Traditional Wood Burning Cookstoves. *Environ. Sci. Technol.* **2006**, *40* (21), 6750–6757. https://doi.org/10.1021/es052080i.

(18) Liu, Z.; Lu, M.; Birch, M. E.; Keener, T. C.; Khang, S. J.; Liang, F. Variations of the Particulate Carbon Distribution from a Nonroad Diesel Generator. *Environ. Sci. Technol.* **2005**, *39* (20), 7840–7844. https://doi.org/10.1021/es048373d.

(19) Roden, C. A.; Bond, T. C.; Conway, S.; Osorto Pinel, A. B.; MacCarty, N.; Still, D.

Laboratory and Field Investigations of Particulate and Carbon Monoxide Emissions from Traditional and Improved Cookstoves. *Atmos. Environ.* **2009**, *43* (6), 1170–1181. https://doi.org/10.1016/j.atmosenv.2008.05.041.

(20) Garland, C.; Delapena, S.; Prasad, R.; L'Orange, C.; Alexander, D.; Johnson, M. Black Carbon Cookstove Emissions: A Field Assessment of 19 Stove/Fuel Combinations. *Atmos. Environ.* **2017**, *169*, 140–149. https://doi.org/10.1016/j.atmosenv.2017.08.040.

(21) Coffey, E. R.; Muvandimwe, D.; Hagar, Y.; Wiedinmyer, C.; Kanyomse, E.; Piedrahita, R.; Dickinson, K. L.; Oduro, A.; Hannigan, M. P. Implications of New Emission Factors and Efficiencies from In-Field Measurements of Traditional and Improved Cookstoves. *Environ. Sci. Technol.* **2017**, *51* (21), 12508–12517. https://doi.org/10.1021/acs.est.7b02436.

(22) Rose Eilenberg, S.; Bilsback, K. R.; Johnson, M.; Kodros, J. K.; Lipsky, E. M.; Naluwagga, A.; Fedak, K. M.; Benka-Coker, M.; Reynolds, B.; Peel, J.; Clark, M.; Shan, M.; Sambandam, S.; L'Orange, C.; Pierce, J. R.; Subramanian, R.; Volckens, J.; Robinson, A. L. Field Measurements of Solid-Fuel Cookstove Emissions from Uncontrolled Cooking in China, Honduras, Uganda, and India. *Atmos. Environ.* **2018**, *190* (March), 116–125. https://doi.org/10.1016/j.atmosenv.2018.06.041.

(23) Grieshop, A. P.; Jain, G.; Sethuraman, K.; Marshall, J. D. Emission Factors of Health- and Climate-Relevant Pollutants Measured in Home during a Carbon-Finance-Approved Cookstove Intervention in Rural India. *GeoHealth* **2017**, *1* (5), 222–236. https://doi.org/10.1002/2017GH000066.

(24) Lefebvre, O. *Household Air Pollution Study Part 1 Black Carbon Emission Factor Measurement for Ethanol Charcoal and Kerosene Stoves in Kibera Kenya*; 2016.

(25) Pokhrel, R. P.; Wagner, N. L.; Langridge, J. M.; Lack, D. A.; Jayarathne, T.; Stone, E. A.; Stockwell, C. E.; Yokelson, R. J.; Murphy, S. M. Parameterization of Single-Scattering Albedo (SSA) and Absorption Ångström Exponent (AAE) with EC/OC for Aerosol Emissions from Biomass Burning. *Atmos. Chem. Phys.* **2016**, *16* (15), 9549–9561. https://doi.org/10.5194/acp-16-9549-2016.